doi:10.14311/ppt.2023.3.146
Plasma Physics and Technology **10**(3):146–149, 2023 © Department of Physics, FEE CTU in Prague, 2023

MOLECULAR DYNAMIC SIMULATION OF EFFECT OF INITIAL SURFACE TEMPERATURE ON ARC EROSION DUE TO ION BOMBARDMENT

X. Wang, S.Y. Matharage, Z.D. Wang *

Centre for Smart Grid, Department of Engineering, University of Exeter EX4 4PY, UK

* zhongdong.wang@exeter.ac.uk

Abstract. This study focuses on the effects of initial surface temperature on arc erosion caused by ion bombardment. The simulation results show that higher surface temperature leads to a greater number of lost Cu atoms and an increased size of the erosion crater. This is due to the ability of the incident ions to have a greater sputtering yield at higher temperatures. Moreover, the Cu atoms tend to agglomerate and form clusters after ion bombardment while leaving the surface.

Keywords: Arc erosion, Ion bombardment, Surface temperature, Molecular dynamics simulation.

1. Introduction

In industrial plasma systems, such as high voltage gas blast circuit breakers (HVCB) and arc plasma generators, one or more electric arcs burn between two solid conductors named electrodes or electrical contacts. The temperature of the arc column can reach as high as 20,000 K due to strong Ohmic heating [1]. Interaction between the arc and the electrical contacts encompasses two primary forms: collisions, characterised by ion bombardment onto the cathode surface, and energy transfer, predominantly through radiation. These dynamic processes lead to the consumption of the contact materials and, subsequently, reduce the circuit breaker's operational lifespan.

The formation of an electric arc can be classified into two distinct cases. Firstly, arc generation occurs during the contacts closing process when the voltage applied across the contacts surpasses the dielectric breakdown voltage or when the distance between the contacts diminishes to a critical threshold [2]. In this case, the arc discharge is initiated through field emission, commonly referred to as "cold emission", and the temperature of the cathode surface remains relatively low before ion bombardment. Secondly, the arc formation takes place during the separation of the contacts. As the arcing contacts begin to open, a molten metal bridge is first formed between the two contacts due to the concentrated heat produced by the current flowing through the interconnected point. The bridge becomes unstable and ruptures as the contacts continue to move apart, releasing the metal vapour into the contact gap space. Consequently, an arc is formed in the metal vapour [3]. In this case, the arc discharge is mainly initiated by thermionic emission, resulting in significantly high cathode surface temperatures before ion bombardment, even surpassing the boiling point of contact materials.

Arc erosion of electrical contact is a complicated process. Understanding the mechanisms behind arc erosion is essential for optimising contact material selection and design. Recently, the application of molecular dynamics (MD) simulations has emerged as a valuable tool for investigating the atomic-level mechanisms underlying arc erosion [4]. Positive ion bombardment of the cathode spot is assumed to be the dominant energy source to maintain the arc cathode spot [5]. By simplifying the arcing process as ion bombardment on cathode surface, [4] revealed mechanisms through which graphene protects Cu from arc erosion in Cu-W arcing contacts from a microscopic level. Results indicated that Cu covered by a graphene layer had fewer vacancies and sputtered atoms than in the pure Cu system, as graphene layer can dissipate the energy transferred from incident ions by shock waves. However, a simplification was made in previous work, where the initial model temperature was set as 300 K. As mentioned above, the temperature of the contact surface before ion bombardment varies depending on the arc formation conditions. Therefore, to further understand the arc erosion mechanisms, it is important to study the effect of the initial temperature of the model surface on arc erosion.

2. Simulation details

This study employs a pure Cu model as the substrate for the ion bombardment simulation, shown in Figure 1(a), as Cu is a widely used material for electrical contacts. The z-direction is subjected to a fixed boundary condition (atoms will be deleted if they move outside the boundary), while periodic boundary conditions are applied in the x and y directions. Furthermore, the three bottom layers in the Cu substrate are fixed to prevent atoms from leaving the box from bottom. The energy minimisation is first performed, and then the model is relaxed at 300 K for 30 ps before bombarding the surface with ions. During ion bombardment, three atom layers at all four vertical faces were forced to maintain 300 K to prevent any waves generated by the bombardment from propagating back through the periodic boundary conditions.

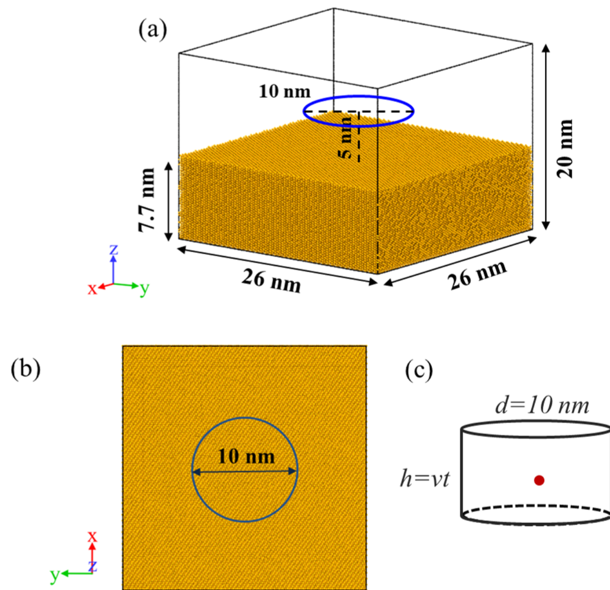

Figure 1. The schematic diagram of the models: (a) pure Cu model. (b) top view of the model. Blue circle shows the incident area. (c) the space independently occupied by each incident ion

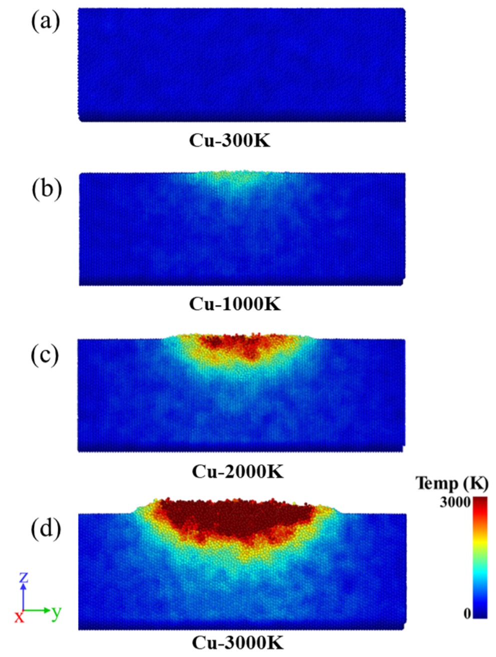

Figure 2. Atomic temperature distribution of the cross-section of four Cu models before ion bombardment.

To adjust the initial temperatures of the models' surfaces, the circle region with a diameter of 10 nm and three-atom-layer thickness on the surface is designated as the "heat source", shown in Figure 1(b). Before ion bombardment, the heat source areas in four models are first heated to the target temperatures (300 K, 1000 K, 2000 K and 3000 K), respectively, and held at that temperature for 30 ps while simultaneously allowing the heat to transfer to the surroundings. Following the heating phase, models are continuously bombarded by 300 sulphur (S) ions from random sites within a cylindrical region with a diameter of 10 nm and a height of 0.5 nm above the model surface. Each incident ion possesses an energy of 50 eV, which incorporates contributions from thermal energy derived from the arc, kinetic energy resulting from the voltage drop in the cathode region, and recombination energy [3, 6]. The time interval between continuous incident atoms is set as 0.1 ps. Figure 1(c) exhibits the space independently occupied by each incident ion. Therefore, the particle density (average number of particles in unit volume) of S ions in the simulation is $7.35 \times 10^{18}\,\mathrm{cm}^{-3}$, which is consistent with the particle density (10^{17} to $10^{18}\,\mathrm{cm}^{-3}$) in [7].

During the ion bombardment process, an NVE (constant Number of particles, Volume, and Energy) ensemble is utilised. The timestep employed in the simulation varies depending on the energy of the incident ions. After the completion of the bombardment, the models are subsequently cooled down to a temperature of 300 K to observe the residual crater. It should be noted that neutral S atoms instead of S ions are used for bombardment in the simulation (the charges of ions are not considered) as ions are neutralised before bombarding the cathode surface [5]. However, an incident particle is still referred to as an "ion", as ion bombardment is a common term in the switching arc research community. Each simulation scenario is repeated five times to identify the statistical deviations in the results.

MD simulations are performed using the Large-scale Atomic/Molecular Massively Parallel Simulator (LAMMPS). The atomic forces between Cu atoms are described by the embedded atom method (EAM) potential, combined with the Ziegler Biersacke Littmark (ZBL) repulsive potential [8]. The atomic forces between the incident S atom with Cu and other S atoms are calculated with the ZBL repulsive potential [9].

3. Simulation Results and Discussion

Figure 2 illustrates the distribution of atomic temperatures in the cross-section of the models following the heating phase, prior to the commencement of ion bombardment. The observed temperature profile exhibits a gradual decrease with increasing depth, indicating the effective transfer of heat from the heat source region towards other directions.

As shown in Figure 2(d), when the surface is subjected to heating at 3000 K, a significant molten pool is formed on the surface. As shown in Figure 3, the simulation reveals the evaporation of Cu atoms from the surface. Based on five repetitions, there were on average 52 Cu atoms evaporated during the heating process set for the surface temperature of 3000 K.

Figure 4 shows the average number of Cu atoms lost in each system after the completion of ion bombardment. This number consists of Cu atoms sputtered away from the model surface by incident ions and those that evaporated when the surface temperature

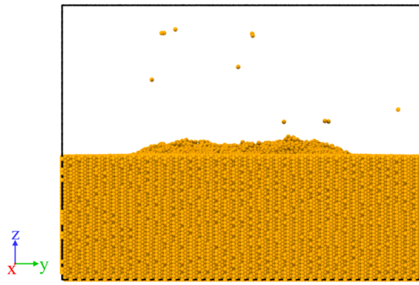

Figure 3. A frame of Cu-3000 K system during heating. The Cu atoms leaving the surface are evaporated atoms.

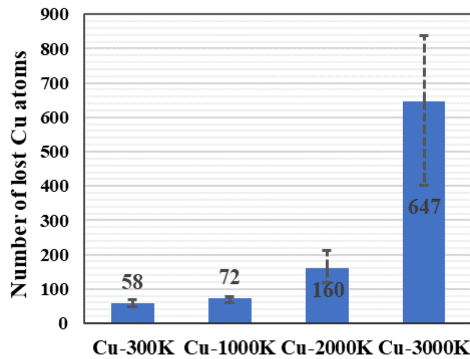

Figure 4. Average number of lost Cu atoms in each system after the completion of ion bombardment.

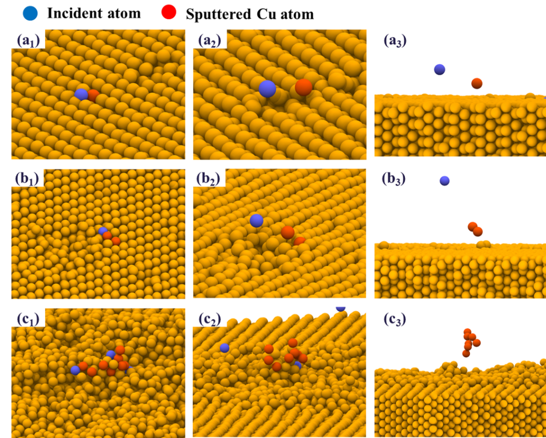

Figure 5. Representative metal atom sputtering processes at different surface temperatures: (a1-a3) Surface temperature is 500 K; (b1-b3) Surface temperature is 900 K; (c1-c3) Surface temperature is 2400 K

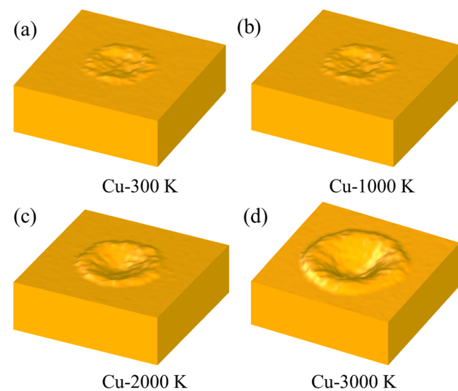

Figure 6. Surface morphologies of Cu models after ion bombardment and being cooled down to 300 K

exceeded the boiling point of Cu (2835 K). According to our observation, the vast majority of lost Cu atoms come from the first cause, especially when the initial surface temperature is below the boiling point of Cu. The data reveals a correlation between the initial surface temperature and the number of lost Cu atoms, with a notable increase when the initial temperature reaches 3000 K. The data can be categorised into three cases: First, when the initial surface temperature is below Cu's melting point (1357 K), the loss of atoms is minimal. Second, when the initial surface temperature is between Cu's melting point and boiling point, a significant increase in the number of lost atoms is observed. Finally, when the initial temperature exceeds Cu's boiling point, there is a sharp escalation in the number of lost Cu atoms.

This phenomenon can be attributed to the sputtering capability of the incident atoms at different surface temperatures. Figure 5 presents the representative metal atom sputtering processes at different surface temperatures. It can be observed that at lower surface temperatures, the incident ions can only cause the ejection of one Cu atom, as shown in Figure 5(a1)–(a3). In order to show the sputtering process of Cu atoms better, the viewing angles and scales in the figures are different. As the surface temperature continues to increase towards the melting point, a single incident ion becomes capable of sputtering two Cu atoms, as shown in Figure 5(b1)–(b3). When the surface temperature approaches the boiling point of Cu, an incident ion can lead to the ejection of multiple Cu atoms in the form of small clusters, shown in Figure 5(c1)–(c3). This demonstrates that the sputtering capability of the incident atoms increases with higher surface temperatures.

In models with relatively low surface temperatures, the initial incident ions are used to heat the surface by increasing the kinetic energy of surface atoms. Hence, when the total number of incident ions remains constant, a lower surface temperature in the model requires a higher proportion of incident ions to participate in the surface heating process until the material reaches its boiling point. Consequently, in the system with an initial temperature of 3000 K, all incident ions are able to sputter Cu atoms on the surface to their maximum capacity, resulting in a significant increase in the number of lost Cu atoms. It is worth noting that as the number of incident particles increases (equivalent to the longer exposure time of the arc at a specific location), the differences in the number of lost atoms between models with different initial temperatures will gradually diminish as the proportion of incident ions used to heat the surface to the total number of incident ions decreases.

Temperature	Diameter (Å)	Depth (Å)
300 K	93.41	6.75
1000 K	99.17	10.59
2000 K	118.02	18.14
3000 K	151.13	34.88

Table 1. Average parameters of erosion craters in different systems

Figure 6 shows the surface morphologies of the models in different systems after ion bombardment and being cooled down to 300 K, revealing that the size of the surface erosion crater enlarges as the initial surface temperature increases. The depths (from crater bottom to the highest point of crater rim) and the outer diameters (the largest width) of the erosion craters are provided in Table 1. It can be seen that when the initial temperature is below Cu's melting point, the erosion crater on the surface exhibits a minimal size. However, as the initial temperature surpasses the boiling point temperature of the material, the erosion crater size undergoes a significant increase.

Furthermore, the MD simulation revealed an intriguing phenomenon following the completion of ion bombardment (equivalent to arc quenching or arc moves to other locations): metal ions leaving the surface gradually aggregate into small clusters, as shown in Figure 7. This is due to the decrease in temperature and kinetic energy of metal atoms without ion bombardment. Therefore, when neighbouring metal atoms approach each other closely, the interatomic interaction forces come into play, resulting in their binding and subsequent formation of small clusters.

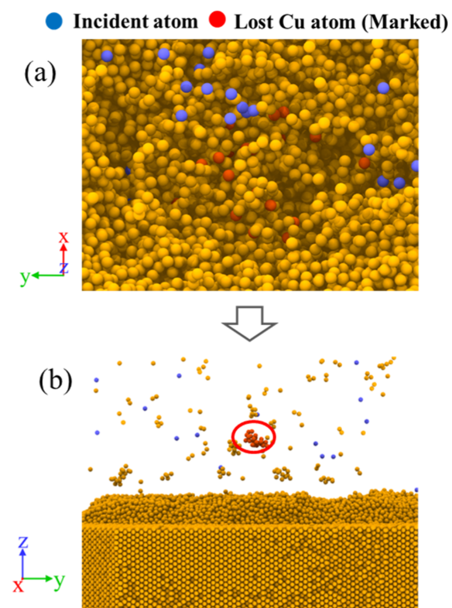

Figure 7. Agglomeration of Cu atoms forming clusters after ion bombardment: (a) marked Cu atoms were inside separately from the top view; (b) marked Cu atoms agglomerated during leave surface, from the side view.

4. Conclusions

The present study focused on exploring the effects of initial surface temperature on arc erosion due to ion bombardment. Simulation results highlight a notable correlation between initial surface temperature and contact erosion. Specifically, higher surface temperatures result in a greater number of lost Cu atoms and an increased size of the erosion crater. This is due to the enhanced sputtering ability of the cathode surface at elevated temperatures with incident ions of the same energy. Additionally, the simulation reveals that Cu atoms tend to agglomerate and form clusters while leaving the surface after ion bombardment.

Overall, this work provides a deeper understanding of ion bombardment across a range of surface temperatures, thereby improving the MD simulation model for arc erosion in diverse arc plasma environments. Consequently, it enables more precise and insightful investigations into the arc erosion process within industrial plasma systems.

Acknowledgements

This work was supported by the State Grid Corporation of China Science and Technology Foundation (5500-201958505A-0-0-00).

References

[1] X. Zhou, J. Heberlein, and E. Pfender. Theoretical study of factors influencing arc erosion of cathode. *IEEE Transactions on Components, Packaging, and Manufacturing Technology: Part A*, 17(1):107–112, 1994. doi:10.1109/95.296375.

[2] W. P. Dyke and J. Trolan. Field emission: Large current densities, space charge, and the vacuum arc. *Physical Review*, 89(4):799, 1953. doi:10.1103/PHYSREV.89.799.

[3] P. G. Slade. *Electrical contacts: principles and applications*. CRC press, 2017. ISBN 978-1-4398-8131-6.

[4] R. Xu, M. Zhou, X. Wang, et al. A molecular dynamics simulation study on the role of graphene in enhancing the arc erosion resistance of Cu metal matrix. *Computational Materials Science*, 212:111549, 2022. doi:10.1016/J.COMMATSCI.2022.111549.

[5] J. Rich. Resistance heating in the arc cathode spot zone. *Journal of Applied Physics*, 32(6):1023–1031, 1961. doi:10.1063/1.1736153.

[6] R. Tang and J. Callaway. Electronic structure of SF6. *The Journal of chemical physics*, 84(12):6854–6860, 1986. doi:10.1063/1.450850.

[7] H. Ito et al. *Switching Equipment*. Springer, 2019. doi:10.1007/978-3-319-72538-3.

[8] M. J. Demkowicz and R. Hoagland. Simulations of collision cascades in Cu–Nb layered composites using an eam interatomic potential. *International Journal of Applied Mechanics*, 1(03):421–442, 2009. doi:10.1142/S1758825109000216.

[9] J. F. Ziegler and J. P. Biersack. *The stopping and range of ions in matter*. Springer, 1985. doi:10.1007/978-1-4615-8103-1_3.